ARTICLE

THz-TDS study on the sulfur doping effect in the properties of $GaSe_{1-x}S_x$

Arvin Lester C. Jusi*[1,3], Der Jun Jang[1], Yi Ying Lu[1], Ching Hwa Ho[2], Li Wei Tu[1], Wen Ching Chao[1], and Alvin Karlo G. Tapia[3]

[1]Department of Physics, National Sun Yat-sen University, Kaohsiung City, Taiwan
[2]Graduate Institute of Applied Science and Technology, National Taiwan University of Science and Technology, Taipei, Taiwan
[3]Institute of Physics, University of the Philippines Los Baños, Los Baños, Laguna, Philippines

ABSTRACT

The optical and electrical properties of $GaSe_{1-x}S_x$ samples in the terahertz range were obtained using terahertz time-domain spectroscopy (THz-TDS). Results showed that the properties of the $GaSe_{1-x}S_x$ samples approach that of GaS as the amount of sulfur increases. This behavior is linked to the stacking type transition of the $GaSe_{1-x}S_x$ samples due to incorporation of sulfur. The THz absorption and conductivity of the $GaSe_{0.9}S_{0.1}$ sample were also observed to be lower than GaSe, but further addition of sulfur has led to the increase of THz absorption and conductivity. The carrier concentration and mobility obtained from Drude fitting of the conductivity have shown consistency with the behavior of the $GaSe_{1-x}S_x$ samples with increasing amounts of sulfur.

*Corresponding author
Email Address: acjusi@up.edu.ph
Date received: April 25, 2024
Date revised: June 26, 2024
Date accepted: July 22, 2024
DOI: https://doi.org/10.54645/2024172RGA-66

INTRODUCTION

From the recent years, gallium selenide (GaSe) has attracted a great deal of attention due to its potential for fabrication of optoelectronics operating in the visible region [1]. A lot of research has been focusing also on GaSe due to its remarkable properties and plenty of modern applications such as superconducting nanoelectronics, flexible optoelectronics [3], and as a multifunctional 2D material [4]. Moreover, GaSe is also a very promising material for far-infrared and THz applications [4-15] due to its extremely low optical losses (<0.1 cm^{-1} in the infrared range), very wide transparency range (0.65–18 μm), and large nonlinear optical coefficient (d_{22}≈70–80 pm/v) [4, 6-11]. However, despite the number of studies with the properties of GaSe, it is still challenging to develop its full potential as a key material in technological devices due to its poor physical properties. The hardness of GaSe is close to zero in the Moh's scale [10,12,13], and the lattice interlayers are held only by very weak van der Waals forces, thus forming high-quality GaSe crystals presents a challenge [14-16].

KEYWORDS

Terahertz time-domain spectroscopy, sulfur-doped GaSe, stacking type transition, THz absorption and conductivity, Drude fitting

Incorporating other chalcogens in GaSe can improve its physical properties due to reduction of stacking faults and filling up of gallium vacancies [15]. Among these chalcogenides previously studied, the incorporation of sulfur proves to be the most advantageous for GaSe [13-23]. Owing to the similarities in the size of sulfur and selenium, it is possible to form $GaSe_{1-x}S_x$ crystals with high concentrations of sulfur [14]. Since the physical properties of GaSe were shown to be proportional to the concentration of the incorporated chalcogenide, the improvements were most remarkable with the incorporation of sulfur [14-16]. This is attributed to the changes in the stacking pattern of the $GaSe_{1-x}S_x$ crystals induced by the addition of sulfur. As shown in Figure 1, the common structure of GaSe at room temperature follows an ε-type stacking pattern while GaS follows a β-type stacking pattern [1]. Thus, the $GaSe_{1-x}S_x$ crystals with low sulfur concentrations have an ε-type stacking and undergo transition to β-type stacking as the sulfur concentration becomes higher [13]. The anions and cations of the succeeding layers are closer in the β-type stacking than in the ε-type stacking, creating an interlayer bonding that is ionic in nature in addition to the van der Waals forces, thus making the interlayer bonding stronger. As a result, $GaSe_{1-x}S_x$ crystals have the largest increase in hardness and optical damage threshold [14]. With the dependence on the amount of sulfur, the properties of $GaSe_{1-x}S_x$ crystals are highly tunable, making them the ideal material for the fabrication of long-pass filters, light emitting devices, and optical detecting systems in the visible region [17]. $GaSe_{1-x}S_x$ crystals also preserve the attractive optical properties of GaSe in the THz region such as large birefringence (0.375) making them more effective in THz emission and detection applications [10, 18-22]. This also leads to $GaSe_{1-x}S_x$ to be more advantageous than other crystals for electro-optic sampling of broadband THz signals [11, 23].

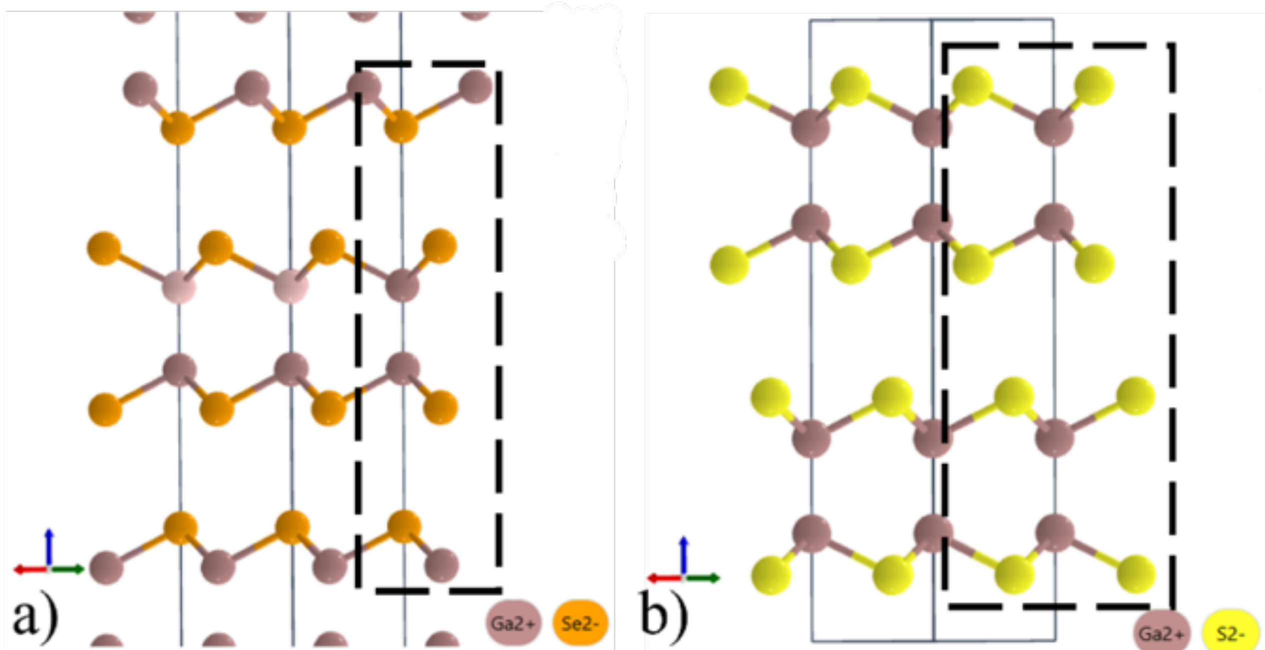

Figure 1: **(a)** ε-type stacking of and GaSe and **(b)** β-type stacking of GaS.

As a new promising multifunctional and nonlinear material, it is essential to investigate the optical properties of $GaSe_{1-x}S_x$ in the THz range to extend its capabilities. The knowledge of its optical and electrical properties in the THz range can serve as foundations for developing applications for $GaSe_{1-x}S_x$. Despite the existence of a number of studies about the optical properties of $GaSe_{1-x}S_x$, a study providing a substantial investigation about its conductivity in the THz region is still lacking. The time scale of charge carrier dynamics in materials, such as relaxation, falls within the ultrafast range (10^{-9} to 10^{-18} s) [24] and can be effectively probed using THz frequency measurement techniques. Hence, understanding the conductivity of the $GaSe_{1-x}S_x$ samples in the THz frequency is important in describing the dynamical responses of charges in $GaSe_{1-x}S_x$. By fitting theoretical models for describing the carrier dynamics of materials to the THz conductivities, the carrier concentration and carrier density can be calculated. In this study, the different THz optical properties and conductivities of $GaSe_{1-x}S_x$ obtained using terahertz time-domain spectroscopy (THz-TDS) will be reported. The carrier concentration and carrier density of the $GaSe_{1-x}S_x$ samples obtained through fitting of the Drude model to the THz conductivities were also reported.

MATERIALS AND METHODS

In this study, we investigated GaSe, GaS, and four $GaSe_{1-x}S_x$ (X=0.1, 0.2, 0.3, 0.5) samples using THz-TDS. GaX (X = S, Se) and $GaSe_{1-x}S_x$ are layered-type dichalcogenide semiconductors [1, 17, 26]. The GaSe and $GaSe_{1-x}S_x$ samples were grown through the vertical Bridgman method while the GaS sample was grown by chemical vapor transport (CVT) using Br_2 as the transport agent [26]. The Se and S concentrations were obtained by determining the chalcogen difference in the grown crystal sample and the nominal starting compositions using electron probe microanalysis, thus, the value of X is defined by the nominal starting composition [1, 17, 26]. A Ti:sapphire laser source was used to generate laser pulses with 100 fs pulse width, 800 nm wavelength, and a repetition rate of 80 MHz. Using a beam splitter, the laser pulses were separated into two beams, namely the pump and the probe. The pump beam was used to generate THz radiation from a semi-insulating low-temperature grown GaAs (LT-GaAs) photoconductive antenna. The THz radiation was focused on the sample using off-axis gold-plated parabolic mirrors. The probe beam was directed to overlap with THz radiation transmitted through the samples to monitor the evolution of the THz radiation in the time domain. The detection mechanism employs the electro-optic sampling method with a ZnTe crystal used as the birefringent crystal. [18, 22, 24, 27]

RESULTS AND DICUSSIONS

The THz properties of the $GaSe_{1-x}S_x$ samples, GaSe, and GaS were successfully obtained. The index of refraction is shown in Fig. 2a (real) and 2b (imaginary). The values were derived by first comparing the obtained spectra of the samples shown in Eq. 1 where $\tilde{E}_{sam}(\omega)$ and $\tilde{E}_{ref}(\omega)$ are the Fast Fourier Transformation of the time-domain signals of the sample and reference, respectively, and then fitting with Eq. 2 where d is the thickness of the sample, c is the velocity of light in vacuum, and $\tilde{n} = n + i\kappa$ will be the calculated complex index of refraction of the samples after fitting [23, 24, 29].

$$\tilde{t}(\omega) = \frac{\tilde{E}_{sam}(\omega)}{\tilde{E}_{ref}(\omega)} \quad (1)$$

$$\tilde{t}(\omega) = \frac{2\tilde{n}(\tilde{n}_{ref}+1)\exp\left[\frac{i\omega(\tilde{n}-1)d}{c}\right]}{(1+\tilde{n})(\tilde{n}+\tilde{n}_{ref})} \cdot \frac{1}{1-(\frac{\tilde{n}-1}{\tilde{n}+1})(\frac{\tilde{n}-\tilde{n}_{ref}}{\tilde{n}+\tilde{n}_{ref}})\exp(2i\omega\tilde{n}d/c)} \quad (2)$$

The refractive indices and the extinction coefficients of the $GaSe_{1-x}S_x$ samples with $0 \leq X \leq 0.5$ only exhibited small shifts in values and show no general trend across the 0.2 – 2.0 THz region. At the 0.8 – 2.0 THz region, both the refractive indices and extinction coefficients of the $GaSe_{1-x}S_x$ samples with $0 \leq X \leq 0.3$ can be observed to have a similar dependence with frequency. Although there is a transition-type stacking (mixture of ε-type and β-type) that is existing in the $GaSe_{1-x}S_x$ samples with $0.1 \leq X \leq 0.3$, the ε-type stacking pattern remains dominant similar to GaSe [1, 17, 26]. The small shifts in values as well as the similarities in the frequency dependence show that incorporating sulfur does not affect considerably the dispersion property of the $GaSe_{1-x}S_x$ samples in the THz range. This is potentially a positive result as it was previously discussed that GaSe is a promising material for THz applications and the addition of sulfur will not cause depreciation of its dispersion properties. On the other hand, in the case of $GaSe_{0.5}S_{0.5}$, the β-type stacking pattern starts to dominate and the behavior can be observed to be starting to follow that of GaS such as the inflection near the 1.5 THz region, albeit less pronounced than GaS [1, 17, 26]. This suggests that increasing the sulfur concentration can lead to GaS-like properties in the $GaSe_{1-x}S_x$ samples.

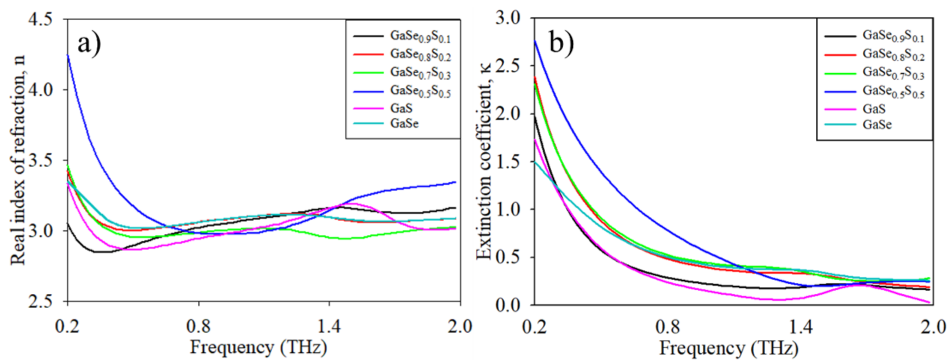

Figure 2: (a) real index of refraction and **(b)** extinction coefficient of the GaSe1-xSx with GaS and GaSe.

The absorption coefficients reported in this study (see Fig. 3a) indicate the existence of an optimal concentration of sulfur. The reduction of the THz absorption is observed in $GaSe_{0.9}S_{0.1}$ having a smaller absorption coefficient than GaSe (see Fig. 3b). In contrast, the absorption coefficients of $GaSe_{0.8}S_{0.2}$ and the other intermediate samples with higher sulfur concentration are larger than GaSe, suggesting that the decrease in the THz absorption can be achieved only up to a certain concentration of sulfur, thus an optimal level. It is clear from Fig. 3 that the optimal sulfur concentration is close to X=0.1. This decrease in the absorption coefficient of the $GaSe_{1-x}S_x$ can be explained by the dependence of the density of states with the incorporation of sulfur [12, 26, 28]. At the optimal sulfur concentration, the density of states is lower, and the phonon-assisted conduction becomes dominant [28]. This is supported by previous studies, where the magnitude of the phonon absorption reaches maximum at the optimal concentration, and the THz absorption will tend to approach its minimum [12, 15, 16]. With further addition of sulfur, the density of states increases, the phonon absorption vanishes, and the THz absorption becomes dominant due to conduction mechanisms [12, 26, 28]. Furthermore, GaS is shown to have lower THz absorption than the $GaSe_{1-x}S_x$ samples ($0 \leq X \leq 0.5$), however, the THz absorption behavior of $GaSe_{0.5}S_{0.5}$ can be seen to follow that of GaS [12, 15, 16].

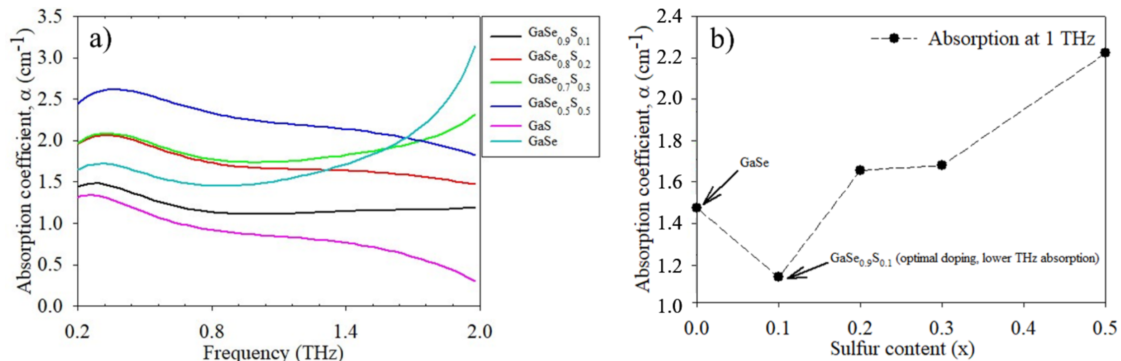

Figure 3: a) Absorption coefficient spectra of the GaSe1-xSx with GaS and GaSe, and **b)** extracted absorption values at 1 THz.

To the best of our knowledge, there is still no study that sufficiently explains the effect of adding sulfur to the THz conductivities of $GaSe_{1-x}S_x$. In this study, the behavior of the THz conductivities is reported, and the carrier dynamics obtained through the Drude model is shown. The complex conductivity can be derived from the index of refraction of the GaSe and $GaSe_{1-x}S_x$ samples [24, 29, 31-33]. Shown in Fig 4(a) and Fig. 4(b) are the real and imaginary conductivities of $GaSe_{1-x}S_x$, respectively. At 0.2 – 1.4 THz, the conductivity of $GaSe_{0.8}S_{0.2}$, $GaSe_{0.7}S_{0.3}$, and $GaSe_{0.5}S_{0.5}$ is larger than the conductivity of GaSe, indicating that increasing sulfur concentrations leads to the increase in conductivity. The increase in conductivity shows strong consistency with the stacking type transition induced by the addition of sulfur.

Samples with transition-type stacking patterns are characterized by large anion vacancies due to the β-polytype areas which increases the mobility of the charge carriers, thus increasing the conductivity [8, 28]. As also previously mentioned, addition of sulfur increases the states density of the conduction band and the valence band resulting to higher THz absorption and higher THz conductivity. However, for GaS (X=1), the overall THz conductivity becomes less than that of the $GaSe_{1-x}S_x$ samples ($0 \leq X \leq 0.5$). This is mainly due to the decrease in carrier concentration in GaS as it will have the same gallium vacancies as GaSe [6, 8, 15, 28].

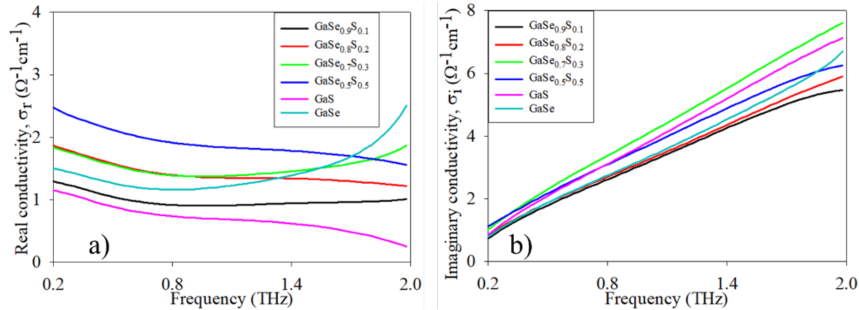

Figure 4: (a) real and **(b)** imaginary conductivity of GaSe1-xSx with GaS and GaSe.

The reported values of THz conductivities of GaSe vary in different studies depending on the technique used, however, since there is still no substantial investigation with the conductivities of $GaSe_{1-x}S_x$ samples, an accepted range of values is still undetermined. The real conductivity of GaSe using THz-TDS has been reported to be in the range of 0.1~0.3 $\Omega^{-1}cm^{-1}$, and the imaginary conductivity is reported within 1-3 $\Omega^{-1}cm^{-1}$ [31, 33]. These values are sufficiently closer to what we have obtained in our study compared to the Hall effect measurement values which are in the 10^{-3} $\Omega^{-1}cm^{-1}$ magnitude [8].

The conductivities can then be fitted with the Drude model to derive the carrier concentration and mobility [24, 29]. The fitted conductivities are shown in Fig. 5. The value of the carrier concentration and carrier mobility can verify the consistency of the behavior of the conductivity of the $GaSe_{1-x}S_x$ samples with the varying amount of sulfur and to the transitioning of the stacking type. The obtained carrier concentration and mobility are shown in Fig. 6. The carrier concentration of the $GaSe_{1-x}S_x$ crystals generally decreases as the sulfur content increases, approaching that of GaS. On the other hand, the carrier mobility increases as the sulfur content increases, but also consistent with the behavior of approaching that of GaS, thus showing agreement with the effect of stacking type transitioning the $GaSe_{1-x}S_x$ samples induced by incorporation of sulfur.

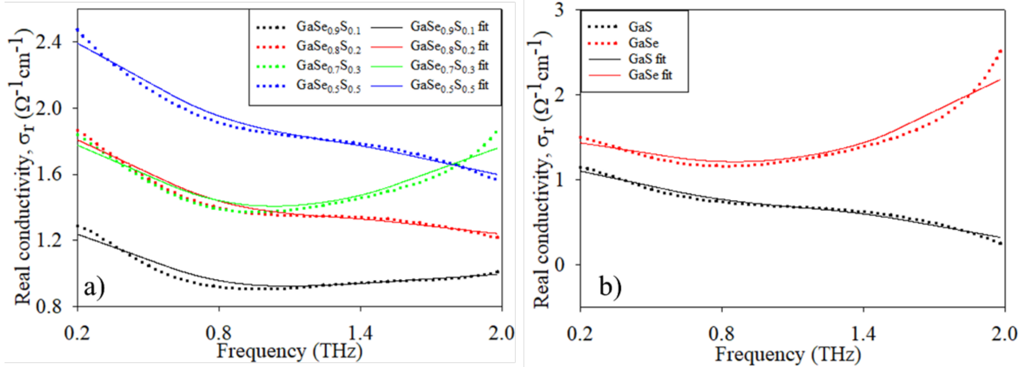

Figure 5: Drude fitting (thin lines) of real conductivity of **(a)** $GaSe_{0.9}S_{0.1}$, and $GaSe_{0.5}S_{0.5}$, and **(b)** GaSe and GaS.

Moreover, Fig. 6 shows consistency with the general trend of the $GaSe_{1-x}S_x$ samples ($0.1 \leq X \leq 0.5$) in Fig. 5a as the samples with higher conductivity have higher carrier mobility. Also, the increase of sulfur concentration caused the existence of the transition-type stacking pattern, which is characterized by large anion vacancies, thus, decreasing the carrier concentration [8, 28].

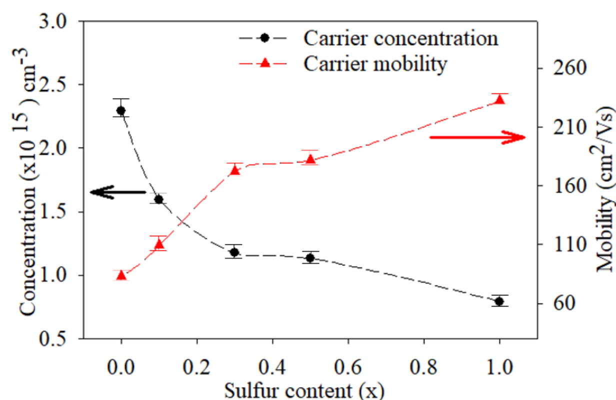

Figure 6: Carrier concentration and mobility of GaSe1-xSx, GaS and GaSe.

Finally, other studies that used Drude model fitting reported a value of the electron mobility value of 89 $cm^2/V{\cdot}s$ and concentration in the 10^{15} cm^{-3} range for GaSe [31, 33], and it can be observed that the values of the carrier concentration and mobility of GaSe reported in Fig. 6 show agreement with these reported values.

CONCLUSION

In conclusion, we reported the complex index of refraction, absorption coefficient, and complex conductivity of the $GaSe_{1-x}S_x$ (X= 0, 0.1, 0.2, 0.3, 0.5, 1) crystals in the THz range. Using simple Drude model fitting, we successfully obtained the carrier concentration and carrier mobility of the samples. The complex index of refraction was seen to have no considerable dependence on sulfur doping. A decrease in the absorption was observed in $GaSe_{0.9}S_{0.1}$ having a smaller absorption coefficient than GaSe, but was seen to increase for X=0.2, 0.3, and 0.5. This suggests that an optimal sulfur concentration exists and is close to X=0.1. Similarly, it was seen that the conductivity increases as the sulfur concentration increases. The increase in conductivity was attributed to the stacking type transition induced by incorporation of sulfur, where the mobility of the carriers increases as the amount of sulfur increases, leading to higher conductivity. Moreover, the obtained carrier mobility and carrier concentration verified the behavior of the $GaSe_{1-x}S_x$ samples approaching GaS-like properties as the sulfur concentration increases.

ACKNOWLEDGMENT

In memory of Dr. Der-Jun Jang, whose invaluable contributions and dedication to this work were instrumental. Their insights and efforts have left a lasting impact on this research, and they are deeply missed.

CONFLICT OF INTEREST

The authors declare no conflict of interest.

CONTRIBUTIONS OF INDIVIDUAL AUTHORS

ALC Jusi and DJ Jang conceptualized the study, performed the experiments, and wrote the manuscript. YY Lu, CH Ho, LW Tu, and AKG Tapia provided expertise to enhance the manuscript. CH Ho also prepared the samples used in this study. WC Chao assisted in the experiments and data gathering.

REFERENCES

Al-Hattab M, Moudou L, Chrafih Y, Rahmani K, Khenfouch M, Bajjou O. First-principles calculation of the structural, electronic, and optical properties of $GaSe_{1-x}S_x$ (x = 0, 0.25, 0.5, 1) compounds. Advances in Materials and Processing Technologies. 2021;13.

Almadvari RH, Nayeri M, Fotoohi S. Engineering of electronic and optical properties of monolayer gallium sulfide/selenide in presence of intrinsic atomic defects. Materials Research Express. 2020;7:015915.

Andreev YM, Atuchin VV, Lanskii GV, Morozov AN, Pokrovsky LD, Sarkisov SY, Voevodina OV. Growth, real structure and applications of $GaSe_{1-x}S_x$ crystals. Materials Science and Engineering B. 2006;128:205–221.

Bereznaya SA, et al. Broadband and narrowband terahertz generation and detection in $GaSe_{1-x}S_x$ crystals. Journal of Optics. 2017;19:115503.

Chen CW, Tang TT, Lin SH, Huang JY, Chang CS, Chung PK, Yen ST, Pan CL. Optical properties and potential applications of ε-GaSe at terahertz frequencies. Journal of the Optical Society of America B. 2009;26(9).

Dmitriev VG, Gurzadyan GG, Nikogosyan DN. Handbook of Nonlinear Optical Crystals. Springer; 1997.

Duvillaret L, Garet F, Coutaz JL. A reliable method for extraction of material parameters in terahertz time-domain spectroscopy. IEEE Journal of Selected Topics in Quantum Electronics. 1996;2:739.

Fernelius NC. Properties of gallium selenide single crystal. Progress in Crystal Growth and Characterization of Materials. 1994;28:275.

Guo H, Zhang X, Liu W, Yong A, Tang S. Terahertz carrier dynamics and dielectric properties of GaN epilayers with different carrier concentrations. Journal of Applied Physics. 2009;106:063104.

Guo J, Xie JJ, Li DJ, Yang GL, Chen F, Wang CR, Zhang LM, Andreev YM, Kokh KA, Lanskii GV, Svetlichnyi VA. Doped GaSe crystals for laser frequency conversion. Light: Science & Applications. 2015;4:e362.

Ho CH, Huang KW. Visible luminescence and structural property of $GaSe_xS_{1-x}$ ($0 \leq x \leq 1$) series layered crystals. Solid State Communications. 2005;136:591.

Ho CH, Wu CC, Cheng ZH. Crystal structure and electronic structure of $GaSe_xS_{1-x}$ series layered solids. Journal of Crystal Growth. 2005;279:321.

Kokh KA, Molloy JF, Naftaly M, Andreev YM, Svetlichnyi VA, Lanskii GV, Lapin IN, Izaak TI, Kokh AE. Growth and optical properties of solid solution crystals $GaSe_{1-x}S_x$. Materials Chemistry and Physics. 2015;154.

Lee YS. Principles of Terahertz Science and Technology. Mainz, Germany: Proceedings of the International Conference; 2009.

Li GF, Huang RJ, Huang JG, Zhang WJ, Cui HY, Xia NH, Huang ZM, Chu JH, Ma GH. Impact of sulfur doping on broadband terahertz emission in gallium selenide single crystals via optical rectification. Applied Physics Express. 2021;14:072004.

Liu K, Xu J, Zhang XC. GaSe crystals for broadband terahertz wave detection. Applied Physics Letters. 2004;85:863.

Molloy JF, Naftaly M, Andreev YM, Kokh KA, Lanskii GV, Svetlichnyi VA. Absorption anisotropy in sulfur-doped gallium selenide crystals studied by THz-TDS. Optical Materials Express. 2014;4(11):2451.

Naftaly M, Molloy JF, Andreev YM, Kokh KA, Lanskii GV, Svetlichnyi VA. Dispersion properties of sulfur-doped gallium selenide crystals studied by THz TDS. Optics Express. 2015;23(25):3282014.

Nazarov MM, Sarkisov SY, Shkurinov AP, Tolbanov OP. $GaSe_{1-x}S_x$ and $GaSe_{1-x}Te_x$ thick crystals for broadband terahertz pulses generation. Applied Physics Letters. 2011;99:081105.

Ni YB, Wu HX, Huang CB, Mao MS, Wang ZY, Cheng XD. Growth and quality of gallium selenide (GaSe) crystals. Journal of Crystal Growth. 2013;381:10.

Palik ED. Handbook of Optical Constants of Solids. Academic Press; 1998.

Rahaman M, Rodriguez RD, Monecke M, Lopez-Rivera SA, Zahn DRT. GaSe oxidation in air: from bulk to monolayers. Semiconductor Science and Technology. 2017;32(10).

Sha T, Li W, Chen S, Jiang K, Zhu J, Hu Z, Huang Z, Chu J, Kokh K, Andreev Y. Effects of S-doping on the electronic transition, band gap, and optical absorption of $GaSe_{1-x}S_x$ single crystals. Journal of Alloys and Compounds. 2017;721:164.

Shi W, Ding YJ, Fernelius N, Vodopyanov K. Efficient, tunable, and coherent 0.18–5.27 THz source based on GaSe crystal. Optics Letters. 2002;27(16):1454.

Singh NB, Su CH, Arnold B, Choa FS, Sova S, Cooper C. Multifunctional 2D-materials: Gallium selenide. Materials Today: Proceedings. 2017;4(4E):5471.

Singh NB, Suhre DR, Balakrishna V, Marable M, Meyer R, Fernelius N, Hopkins FK, Zelmon D. Far infrared conversion materials: gallium selenide for far infrared conversion applications. Progress in Crystal Growth and Characterization of Materials. 1998;47.

Skjeie HCB. Terahertz Time-Domain Spectroscopy. Norwegian University of Science and Technology; 2012.

Ueno K, Abe H, Saiki K, Koma A. Heteroepitaxy of layered semiconductor GaSe on a GaAs(111)B surface. Japanese Journal of Applied Physics. 1991;30(8A):L1352.

Voevodina OV, Morozov AN, Sarkisov SY, Bereznaya SA, Korotchenko ZV, Dikov DE. Properties of gallium selenide doped with sulfur from melt and from gas phase. Proceedings of the 9th Russian-Korean International Symposium on Science and Technology. 2005;551.

Wu CC, Ho CH, Shen WT, Huang YS, Tiong KK. Optical properties of $GaSe_xS_{1-x}$ series layered semiconductors grown by vertical Bridgman method. Materials Chemistry and Physics. 2004;88:313.

Yu BL, Altan H, Zeng F, Kartazayev V, Alfano RR, Mandal KC. Terahertz resonances in the dielectric response due to second-order phonons in a GaSe crystal. Materials Research Society Proceedings. 2006;935:0935-K03-08.

Yu BL, Zeng F, Kartazayev V, Alfano RR. Terahertz studies of the dielectric response and second-order phonons in a GaSe crystal. Applied Physics Letters. 2005;87:182104.

Zhang W, Azad AK, Grischkowsky D. Terahertz studies of carrier dynamics and dielectric response of n-type, freestanding epitaxial GaN. Applied Physics Letters. 2003;82:2841.